

# New insights on the role of sea ice in intercepting atmospheric pollutants using $^{129}\text{I}$

J.M. Gómez-Guzmán<sup>a,\*</sup>, P. Cámara-Mor<sup>b</sup>, T. Suzuki<sup>c</sup>, J.M. López-Gutiérrez<sup>a,d</sup>, J.L. Mas<sup>d</sup>, P. Masqué<sup>b,e,f</sup>, S.B. Moran<sup>g</sup>, J.N. Smith<sup>h</sup>

<sup>a</sup> Centro Nacional de Aceleradores (CNA), Avda. Thomas alba Edison 7, Isla de la Cartuja, 41092 Sevilla, Spain

<sup>b</sup> Departament de Física & Institut de Ciència i Tecnologia Ambientals, Universitat Autònoma de Barcelona, Bellaterra, Spain

<sup>c</sup> Reserch Group for Environmental Science, Japan Atomic Energy Agency, 2-4 Shirakata-shirane, Tokai, Ibaraki 319-1195, Japan

<sup>d</sup> Dpto. de Física Aplicada I, Escuela Universitaria Politécnica, University of Sevilla, Spain

<sup>e</sup> Oceans Institute & School of Physics, The University of Western Australia, 35 Stirling Highway, Crawley, WA 6009, Australia

<sup>f</sup> School of Natural Sciences & Centre for Marine Ecosystems Research, Edith Cowan University, Joondalup, WA, Australia

<sup>g</sup> Graduate School of Oceanography, University of Rhode Island, Narragansett, RI 02882-1197, USA

<sup>h</sup> Bedford Institute of Oceanography, Fisheries and Oceans Canada, Dartmouth, NS B2Y 4A2, Canada

## ARTICLE INFO

### Article history:

Available online 23 October 2014

### Keywords:

AMS  
Iodine-129  
Arctic Ocean  
Sea ice  
Atmospheric deposition  
Reprocessing

## ABSTRACT

Measurements of  $^{129}\text{I}$  carried out on sea ice samples collected in the central Arctic Ocean in 2007 revealed relatively high levels in the range of  $100\text{--}1400 \times 10^7$  at  $\text{L}^{-1}$  that are comparable to levels measured in the surface mixed layer of the ocean at the same time. The  $^{129}\text{I}/^{127}\text{I}$  ratio in sea ice is much greater than that in the underlying water, indicating that the  $^{129}\text{I}$  inventory in sea ice cannot be supported by direct uptake from seawater or by iodine volatilization from proximal (nearby) oceanic regimes. Instead, it is proposed that most of the  $^{129}\text{I}$  inventory in the sea ice is derived from direct atmospheric transport from European nuclear fuel reprocessing plants at Sellafield and Cap La Hague. This hypothesis is supported by back trajectory simulations indicating that volume elements of air originating in the Sellafield/La Hague regions would have been present at arctic sampling stations coincident with sampling collection.

## 1. Introduction

Oceanic discharges of anthropogenic radionuclides from European nuclear fuel reprocessing plants (mainly Sellafield and La Hague) have introduced a suite of radionuclide contaminants to the marine environment (eg.  $^{137}\text{Cs}$ ,  $^{90}\text{Sr}$ ,  $^{99}\text{Tc}$ ,  $^{236}\text{U}$ , Pu isotopes and  $^{129}\text{I}$  (AMAP, 2004)) that are useful as tracers for detailed investigations of ocean processes. These studies include surface circulation and mixing in the Nordic Seas (Alfimov et al., 2013), surface and intermediate circulation in the Arctic Ocean (Karcher et al., 2012; Smith et al., 2011) and in the North Atlantic (Casacuberta et al., 2014), and the descent of the dense overflows from the Greenland and Norwegian Seas into the deep North Atlantic (Orre et al., 2010).

The Arctic Ocean is covered by seasonal sea ice that plays an important role in the global and regional climate system, as well

as in the oceanic circulation. Sea ice is formed during winter, mostly on the shallow continental shelves of the Laptev, the Kara and the Barents Seas (Aagaard, 1981). The drifting of sea ice is governed by the Transpolar Drift (TPD) over the Eurasian Basin and the anticyclonic Beaufort Gyre in the Canadian Basin (Barrie et al., 1998). Different chemical species, including radionuclides, can be incorporated into the sea ice through direct input (uptake from seawater during its formation and interception of atmospheric dry and wet deposition). For example, Cámara-Mor et al. (2011) determined that Arctic sea ice can intercept a significant fraction  $30\% \pm 18\%$  of the atmospheric inputs of the cosmogenic radionuclide  $^7\text{Be}$ , depending on the sea ice coverage, and suggested that other contaminants could be similarly accumulated via atmospheric pathways. Chemical substances can also accumulate in sea ice through indirect inputs by uptake from sediments and biota such as algae entrained into the ice. As sea ice reaches ablation areas such as the Fram Strait and, to a lesser degree, the Canadian archipelago, it melts and releases the incorporated chemical species, including radionuclides, to the surface water (Pfirman et al., 1997; Rigor et al., 2002; Masqué et al., 2003). Hence, sea ice has been identified as playing a potentially important role in the

\* Corresponding author at: Technische Universität München, Physics Department E12, James-Franck-Strasse 1, D-85748 Garching bei München, Germany.

E-mail addresses: [jm\\_gomez@us.es](mailto:jm_gomez@us.es), [jose.gomez@ph.tum.de](mailto:jose.gomez@ph.tum.de) (J.M. Gómez-Guzmán).

redistribution and transport of those chemical species in the Arctic Ocean (Masqué et al., 2003, 2007; Cámara-Mor et al., 2010).

$^{129}\text{I}$  is a highly soluble and long-lived ( $T_{1/2} = 15.7 \times 10^6$  years) radionuclide that has been extensively discharged to the environment since the beginning of the nuclear era. Although large amounts of this radionuclide were released during atmospheric nuclear weapons tests and the Chernobyl accident (Raisbeck et al., 1995; Wagner et al., 1996; Gallagher et al., 2005), nuclear fuel reprocessing plants, especially Sellafield (UK) and La Hague (France), are the main sources responsible for recent  $^{129}\text{I}$  increases in the environment. These plants were discharging to the sea about  $20 \text{ kg year}^{-1}$  ( $9.34 \times 10^{25}$  atoms, 13.2 GBq) between 1965 and the beginning of the 1990's. Later, the releases increased up to  $300 \text{ kg year}^{-1}$  ( $1.40 \times 10^{27}$  atoms, 198 GBq), mainly from La Hague (López-Gutiérrez et al., 2004; UNSCEAR, 2000). There is some evidence suggesting that contaminated Russian rivers from Siberia can also be a source of  $^{129}\text{I}$ , but this contribution is nevertheless of minor importance for the large scale distribution of  $^{129}\text{I}$  in the north Atlantic and the Arctic Oceans (Cooper et al., 2001; Cochran et al., 2000).

It has been shown that coastal currents transport  $^{129}\text{I}$  from the Irish Sea and the English Channel to the North Sea and the Arctic Ocean along the Norwegian coast (Raisbeck et al., 1995) (Fig. 1). In the Arctic Ocean,  $^{129}\text{I}$  concentrations can be more than an order

of magnitude higher in Atlantic-origin waters compared to Pacific-origin water, and as a result there is a pronounced tracer front between waters of Pacific and Atlantic origin in the Arctic Ocean (Smith et al., 1998, 1999). Transit times of contaminants in surface water to the Arctic Ocean from the North Sea are 2–4 year to the Barents Sea, 9–10 year to the North Pole and greater than 14 year to the Canada Basin (Dahlgard, 1995; Smith et al., 1999, 2011; Buraglio et al., 1999; Alfimov et al. 2004).

Due to its high solubility in seawater,  $^{129}\text{I}$  concentrations in seawater reflect the general circulation patterns of the different water masses (Orre et al., 2010; Alfimov et al., 2004). Hence, in the Nansen basin  $^{129}\text{I}$  is found predominantly in the upper part (0–500 m) of Atlantic-origin water, reflecting the water mass supply corresponding to the Fram Strait water branch, whereas in the Amundsen basin  $^{129}\text{I}$  is distributed deeper, down to 1000 m, reflecting an additional input of  $^{129}\text{I}$  labelled water from the Barents Sea (Barents Sea Branch Water) (Alfimov et al., 2004; Smith et al., 2011).

Kieser et al. (2005) reported elevated concentrations of  $^{129}\text{I}$  in the range of  $(80\text{--}140) \times 10^5 \text{ atoms m}^{-3}$  in air filters collected along Canada in 1981–1983. In that case, back trajectory analysis of air parcels showed transport from Europe and Russia before arriving to Canada and the Arctic Ocean, and indicated a consistent origin over nuclear processing sites east of the Urals, presumably

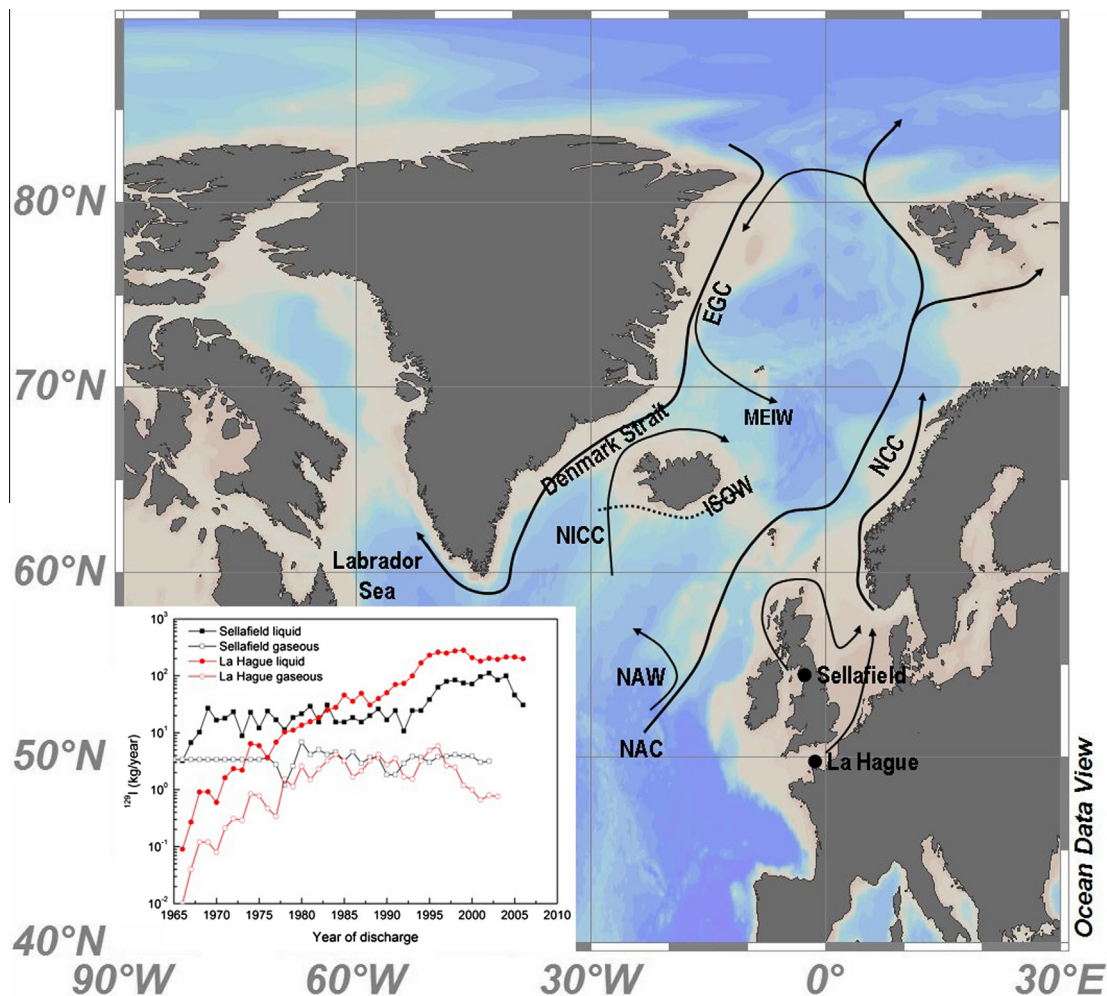


**Fig. 1.** Map showing the major pathways of marine discharges from Sellafield and La Hague nuclear reprocessing facilities to the Arctic and North Atlantic Oceans. Solid lines = surface currents, dashed lines = deep currents, LS = Labrador Sea, NCC = Norwegian Coastal Current, EGC = East Greenland Current, ISOW = Iceland-Scotland Overflow Water, NAC = North Atlantic Current, NAW = North Atlantic Water, NIIC = North Icelandic Irminger Current, MEIW = Modified East Icelandic Water. Inset shows history of  $^{129}\text{I}$  liquid and gaseous discharges (kg/y) from Sellafield (black line) and La Hague (red line) Data extracted from López-Gutiérrez et al. (2004) and He et al. (2013). (For interpretation of the references to colour in this figure legend, the reader is referred to the web version of this article.)

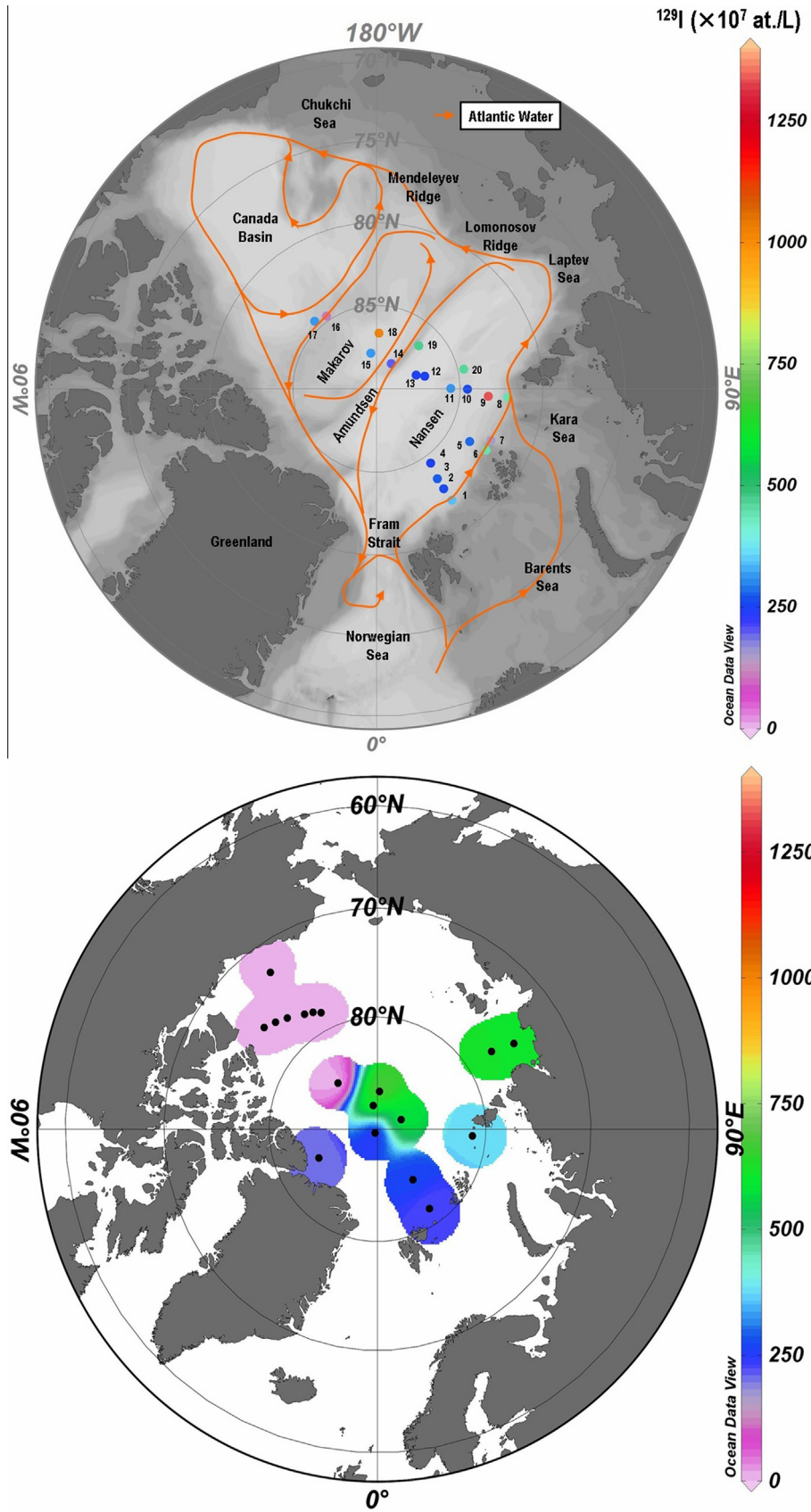


Fig. 2. Up: Geographical distribution of  $^{129}\text{I}$  concentrations measured in sea ice samples collected in the Arctic Ocean during expedition ARK XXII/2-IPY-SPACE in 2007. Map also shows the general circulation of Atlantic and Arctic surface water masses. Bottom: the distribution  $^{129}\text{I}$  in surface seawater samples as measured by Karcher et al. (2012) and Smith et al. (2011).



associated with emissions of atmospheric  $^{129}\text{I}$ . These results indicated that both atmospheric and direct wastewater releases to the ocean from fuel reprocessing plants might be considered as possible sources of  $^{129}\text{I}$  in the Arctic Ocean environment (Snyder et al., 2010; Herod et al., 2013).

The only natural stable isotope of iodine is  $^{127}\text{I}$ . The marine environment is the major source of iodine present on the Earth's surface, with an average concentration of  $\sim 60 \mu\text{g L}^{-1}$  in seawater. Although iodine isotopes ( $^{129}\text{I}$  and  $^{127}\text{I}$ ) are released to the environment in their gaseous forms, they tend to attach to other particles as, e.g. sulphur (Maryon et al., 1991) and their effective dry deposition velocities tend to decrease with time. Wet deposition has been reported to be the major atmospheric removal process and a significant source of radioactive contamination in Northern Europe (Brant et al., 2002; Englund et al., 2010). Although the anthropogenic sources of  $^{129}\text{I}$  to the environment are well known, the anthropogenic emission mechanisms of  $^{127}\text{I}$  are not so clear. Presently, we have no data about anthropogenic sources of  $^{127}\text{I}$  within Europe, but fossil fuel and biomass burning may provide insignificant amounts compared with natural sources (ocean, wetlands, soil and vegetation) (Aldahan et al., 2009).

Much of the Arctic Ocean is ice covered and thus  $^{129}\text{I}$  emission from the water column is highly limited. However, the emission of  $^{129}\text{I}$  from ice free ocean waters enriched in  $^{129}\text{I}$  is still a potential source for the  $^{129}\text{I}$  found elsewhere in the Arctic Ocean. Indeed, it is estimated that approximately  $3.53 \times 10^{25}$  atoms of  $^{129}\text{I}$  (5 GBq) are volatilised from the global oceans every year (Snyder et al., 2010), and Reithmeier et al. (2010) estimate that the total  $^{129}\text{I}$  activity re-emitted from the ocean's surface up to 2004 had been of around 180 GBq. Although the  $^{129}\text{I}$  annually re-emitted reported by Reithmeier et al. (2007) is less than about 0.3% of the  $^{129}\text{I}$  inventory in the upper layer of the ocean, its contribution to the tropospheric  $^{129}\text{I}$  inventory is presently comparable to that from the gaseous releases from Sellafield and La Hague (Fig. 1). A fraction of this  $^{129}\text{I}$  can be carried to the Arctic Ocean via atmospheric transport and is deposited both as dry fallout and with precipitation.

The role of the Arctic sea ice in the transport and biogeochemical partitioning of  $^{129}\text{I}$  and other atmospheric/water mass tracers is still poorly understood. Results of measurements of  $^{129}\text{I}$  in Arctic sea ice are reported in this paper and compared with water column measurements in order to resolve the mechanisms governing  $^{129}\text{I}$  uptake and release from sea ice and to estimate  $^{127}\text{I}$  and  $^{129}\text{I}$  deposition fluxes in the Arctic Ocean.

## 2. Methods and sampling

### 2.1. Sampling

The study area comprises the Eurasian Basin of the Arctic Ocean, from the shelves of the Barents, the Kara and the Laptev Seas across the Nansen, the Amundsen and the Makarov Basins beyond the Alpha Ridge and the Canada Basin (Fig. 2). A total of 20 samples of surface sea ice were collected during the expedition ARK XXII/2-IPY-SPACE of the German R/V Polarstern from July 28 to October 7, 2007 at locations indicated in Fig. 2, located at distances of about 200 m away from the ship. Superficial snow was removed and approximately 100 L of ice from the upper 10 cm were collected by scraping with stain-steel shovels and/or ice-hammer. Once onboard, sea ice was melted at room temperature and samples were stored in polyethylene bottles, in darkness and inside a fridge for 3 years before chemical treatment and analysis of  $^{129}\text{I}$  and  $^{127}\text{I}$ . These storage conditions do not introduce significant changes in the  $^{129}\text{I}$  concentration, as reported by Buraglio et al. (2000). Further details about the samples are given by Cámara-Mor et al. (2011).

### 2.2. Radiochemical procedure

Iodine extraction from sea ice samples was carried out by the solvent extraction technique (Suzuki et al., 2008). Each melted sea ice sample (200 mL) was passed through a  $0.45 \mu\text{m}$  filter and then iodate was reduced to iodide using ascorbic acid and hydrochloric acid. Since the iodine concentration in the samples is too low to measure the isotopic ratio  $^{129}\text{I}/^{127}\text{I}$  by AMS (Accelerator Mass Spectrometry), iodide carrier (2 mg) was added to each sample. Iodide was oxidized to molecular iodine by sodium nitrite and extracted three times with 10 mL chloroform and then the molecular iodine was back-extracted into aqueous solution by addition of 20 mL 0.1 M sodium sulphite. The solution was then stirred and the  $\text{SO}_3^{2-}$  and  $\text{SO}_4^{2-}$  ions were precipitated by addition of 10 mL of saturated  $\text{Ba}(\text{NO}_3)_2$  solution followed by centrifugation. Finally, iodide was precipitated as silver iodide by the addition of 10 mL 0.1 M silver nitrate solution. Silver nitrate was washed with ammonia solution and distilled water. After drying, it was mixed with niobium powder (AgI:Nb = 1:1) and then loaded into a copper target for AMS measurement. Before the addition of the iodide carrier to the samples, an aliquot of each was extracted and used to measure the  $^{127}\text{I}$  concentration by ICP-MS (Inductively Coupled Plasma Mass Spectrometry), as will be explained in Section 2.4.

### 2.3. Measurement of $^{129}\text{I}$ by AMS

Determination of  $^{129}\text{I}$  concentrations was conducted at the 1 MV multielement compact AMS system at the Centro Nacional de Aceleradores (University of Seville). Details about the measurement and the system have been previously described (Gómez-Guzmán et al., 2012), and thus only a brief description is given here. A beam of negative iodine ions is extracted from the AgI + Nb target using the  $\text{Cs}^+$  high-intensity sputter source at 35 keV. At the terminal of the tandem (1 MV) negative iodine ions are changed to positive iodine ions by the stripper (pressure at  $6 \times 10^{-3}$  mbar of argon, which corresponds to a mass thickness of about  $0.15 \mu\text{g cm}^{-2}$ ) and they are then accelerated. Following acceleration, selected positive ions (charge state +3) are analyzed by mass spectrometer.

The sequential injection of  $^{127}\text{I}$  and  $^{129}\text{I}$  is adapted for the isotopic ratio measurement such that the duration of injection is 0.1 ms and 10 ms, respectively. The  $^{127}\text{I}^{3+}$  current beam is measured at the offset faraday cup after the high energy analyzing magnet, and  $^{129}\text{I}^{n+}$  ions are counted in the gas ionization detector. AMS measurements were performed relative to a standard with a known  $^{129}\text{I}/^{127}\text{I}$  isotopic ratio, which was made by repeated dilutions from NIST SRM 3230 Iodine Isotopic Standard Level I.

The isotopic ratios obtained directly by AMS measurement of the samples (including carrier) were typically of the order of  $^{129}\text{I}/^{127}\text{I} \sim 10^{-10}$ – $10^{-11}$ . Chemical blanks to control contamination in the sample preparation process were prepared in exactly the same way as real samples but using deionised water (18 M $\Omega$  cm). The AMS  $^{129}\text{I}/^{127}\text{I}$  ratios for the blanks were around  $3$ – $4 \times 10^{-13}$ , i.e. of about 2–3 orders of magnitude lower than the isotopic ratios measured for the real samples.

### 2.4. Measurement of $^{127}\text{I}$ by ICP-MS

A small aliquot of each sample was taken for analysis of  $^{127}\text{I}$ . After filtering, the samples were diluted 1:2 (v:v) in 1%  $\text{HNO}_3$  and measured by an ICP-MS system Agilent 7500C at the Servicio de Radioisótopos (University of Seville). Measurements were made accordingly to the USEPA 200.8 protocol, excepting that washing between samples was performed by sequentially aspirating deionised water and diluted  $\text{HNO}_3$  instead of just  $\text{HNO}_3$  in order to minimize the intense memory effects of iodine within the ICP-MS

**Table 1**  
Concentration of  $^{129}\text{I}$  in sea ice samples collected during cruise ARKII/2-IPY-SPACE in 2007 in the Arctic Ocean. Quoted uncertainties are  $\pm 1\sigma$ .

No.	Station	Date	Latitude ( $^{\circ}\text{N}$ )	Longitude ( $^{\circ}\text{E}$ )	$^{129}\text{I}$ ( $\times 10^7$ atoms $\text{L}^{-1}$ )
1	PS70/248	02 Aug	81.952	34.076	$332 \pm 39$
2	Helistation	04 Aug	82.792	33.750	$251 \pm 24$
3	PS70/257	05 Aug	83.505	33.973	$267 \pm 23$
4	PS70/260	06 Aug	84.505	36.085	$240 \pm 22$
5	PS70/264	12 Aug	83.608	60.395	$277 \pm 28$
6	PS70/271	15 Aug	82.502	60.791	$434 \pm 24$
7	Helistation	18 Aug	82.502	65.756	$146 \pm 21$
8	PS70/285	20 Aug	82.143	86.320	$434 \pm 24$
9	Helistation	22 Aug	83.296	86.189	$1327 \pm 116$
10	PS70/301	24 Aug	84.563	89.764	$250 \pm 18$
11	Helistation	25 Aug	85.565	90.439	$305 \pm 27$
12	PS70/309	27 Aug	87.034	104.972	$241 \pm 17$
13	Helistation	28 Aug	87.498	109.556	$240 \pm 19$
14	PS70/322	31 Aug	88.254	150.134	$188 \pm 15$
15	PS70/328	02 Sep	87.827	-170.321	$307 \pm 22$
16	PS70/338	05 Sep	84.694	-145.429	$98 \pm 8$
17	PS70/342	07 Sep	84.499	-137.611	$306 \pm 28$
18	PS70/352	10 Sep	86.642	177.545	$1012 \pm 59$
19	PS70/363	13 Sep	86.393	135.817	$461 \pm 36$
20	PS70/371	16 Sep	84.677	102.779	$451 \pm 25$

instrument. The limit of detection was  $0.24 \text{ ng mL}^{-1}$ . As shown below, only two samples produced concentrations above this level.

### 3. Results

The geographical distribution of  $^{129}\text{I}$  concentrations in the surface sea ice samples collected in the Arctic Ocean is shown in Fig. 2 and listed in Table 1. Concentrations ranged between  $(98 \pm 8) \times 10^7$  atoms  $\text{L}^{-1}$  (sample 16) and  $(1327 \pm 116) \times 10^7$  atoms  $\text{L}^{-1}$  (sample 9), with a mean value of  $(378 \pm 292) \times 10^7$  atoms  $\text{L}^{-1}$ . The data were divided into groups according to the sampling regions (i.e. Makarov and Nansen basins). Those belonging to the Makarov basin do not follow a normal distribution; hence a Kruskal–Wallis test (not shown) was applied in order to compare the data distribution medians. No differences were found at the 0.95 significance level between the medians of the three data sets. Relative maxima appear at the Makarov basin (sample 18) and the Nansen basin (sample 9, located near the ridge of the Nansen basin).

Published data on  $^{129}\text{I}$  distributions in sea ice is extremely limited. To our knowledge, the only  $^{129}\text{I}$  concentrations in sea ice samples have been reported by Aldahan et al. (2007), measured at different depths in sea ice cores collected across the Fram Strait during May 2002. Reported concentrations ranged from  $(53.2 \pm 3.7) \times 10^7$  atoms  $\text{L}^{-1}$  at 0–20 cm depth to  $(36 \pm 2) \times 10^7$  atoms  $\text{L}^{-1}$  at 120–140 cm depth of an ice core collected at  $81.96^{\circ}\text{N}$ – $14.11^{\circ}\text{E}$ , and from  $(36 \pm 3) \times 10^7$  atoms  $\text{L}^{-1}$  at 40–60 cm depth to  $(16.6 \pm 1.2) \times 10^7$  atoms  $\text{L}^{-1}$  at 300–320 cm depth of an ice core collected at  $81.44^{\circ}\text{N}$ – $4.07^{\circ}\text{W}$ . In both cases the  $^{129}\text{I}$  concentration in the sea ice core decreased with depth (factors 1.5 and 2, respectively). Based on those results the authors concluded that sea ice would make only a small contribution to the total inventory of  $^{129}\text{I}$  in the Arctic Ocean and related seas (the Nordic, the Barents and the Labrador Seas).

Concentrations of  $^{127}\text{I}$  in the sea ice samples were systematically below the limit of detection ( $0.24 \text{ ng g}^{-1}$ ), with the exception of two samples (1 and 3), with values of  $0.761 \pm 0.020 \text{ ng g}^{-1}$  and  $0.306 \pm 0.025 \text{ ng g}^{-1}$  respectively (average  $0.53 \pm 0.32 \text{ ng g}^{-1}$ ).

### 4. Discussion

Sea ice can incorporate atmospheric fluxes of contaminants (such as radionuclides) and other chemical species. Incorporation during sea ice formation would be negligible because sea ice excludes solutes from the water column during its formation.

Where data are available, an approach that could be used to estimate an order of magnitude of the deposition fluxes of iodine ( $^{129}\text{I}$  and  $^{127}\text{I}$ ) in the Arctic sea ice is to assume that iodine present in sea ice is the balance of iodine deposited by wet or dry deposition as aerosols, iodine incorporated directly by the sea ice from the surrounding seawater, and iodine released from sea ice through different mechanisms.

This approach could then be used to determine the origin of the iodine present in the Arctic sea ice. In the following sections the inventories of both iodine isotopes in the different Arctic environmental compartments are estimated and the mechanisms that govern the fluxes of incorporation/release are discussed in detail.

#### 4.1. Iodine inventory in the Arctic sea ice

As shown by Aldahan et al. (2007), the  $^{129}\text{I}$  concentrations measured in sea ice cores collected across the Fram Strait decreases slightly with depth (factors between 1.5 and 2), so it is reasonable to use the  $^{129}\text{I}$  concentration in surface sea ice samples to calculate the depth inventory in sea ice. Taking the measured concentrations of  $^{129}\text{I}$  and the sea ice thicknesses of the sampled sea ice floes considered here (1.2–2.3 m) (Cámara-Mor et al., 2011), the inventories in sea ice would range from 3.6 to  $20 \times 10^{12}$  atoms  $\text{m}^{-2}$ , with a mean value of  $(6.5 \pm 4.5) \times 10^{12}$  atoms  $\text{m}^{-2}$ . A similar calculation for  $^{127}\text{I}$  (measured in two samples) gives an inventory in the sea ice ranging from 2.6 to  $8.3 \times 10^{18}$  atoms  $\text{m}^{-2}$ , with a mean value of  $(5.5 \pm 4.0) \times 10^{18}$  atoms  $\text{m}^{-2}$ . Those two results lead to a mean  $^{129}\text{I}/^{127}\text{I}$  ratio in the Arctic sea ice samples of  $(1.2 \pm 1.7) \times 10^{-6}$ .

#### 4.2. Iodine inventory in the Arctic mixed layer

The elevated concentrations of  $^{129}\text{I}$  in many parts of the North Atlantic and the Arctic Oceans, particularly in the surface layers of the water column (Orre et al., 2010; Buraglio et al., 2000) has been linked to several anthropogenic sources including nuclear weapons testing, nuclear accidents, dumping of nuclear waste and discharges from nuclear reprocessing facilities (Sellafield and La Hague). The discharges from Sellafield and La Hague are the dominant sources, accounting for >95% of the total inventory in the global ocean until 2000 (Alfimov et al., 2006). It has been well established that the discharged radioactive effluents from the reprocessing facilities at La Hague are transferred northwards to the coast of north-western Europe via the English Channel, mix

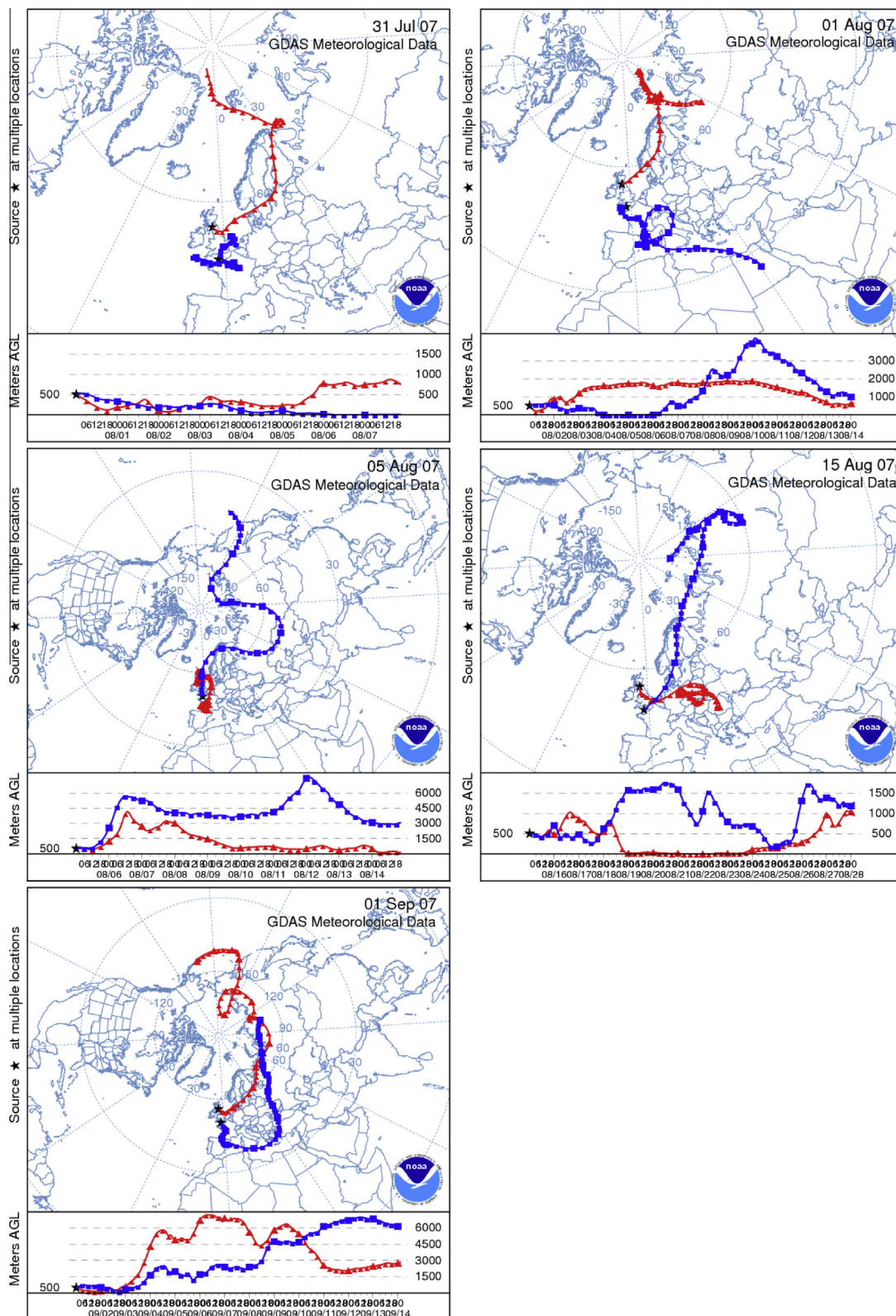


**Fig. 3.** NOAA HYSPPLIT examples of forward-trajectories for air parcels originating at Sellafield (red) and La Hague (blue) between July, 31st 2007 and September, 1st 2007. Note that forward-trajectories are computed at 5-h intervals spanning the 315-h period (the longest provided by the software) starting at 00:00 UTC on the date given. Those trajectories cover the whole sampling period. The lower part of the figures shows the changes in the vertical movement of the air mass trajectories. (For interpretation of the references to colour in this figure legend, the reader is referred to the web version of this article.)

with effluents from Sellafield in the North Sea, and are then further transported by the Norwegian Coastal Current (NCC) to the Arctic Ocean (Alfimov et al., 2004). The inflow of  $^{129}\text{I}$  to the Arctic Ocean occurs via the  $^{129}\text{I}$ -enriched surface branch of the North Atlantic

Current (NAC) and the North Sea water masses along the Norwegian coast (Gascard et al., 2004). In fact, Alfimov et al. (2004) estimated that until 2001 as much as 45% of the maximum possible amount of liquid  $^{129}\text{I}$  from the Western Europe reprocess-



**Table 2**  
Comparison of  $^{129}\text{I}$  and  $^{127}\text{I}$  deposition fluxes measured worldwide. Those  $^{129}\text{I}$  deposition values with (\*) are not measured but calculated by Reithmeier et al. (2010) and corrected for the corresponding local precipitation rates.

No.	Sampling Station	Date	Sample	$^{129}\text{I}$ deposition ( $\times 10^{12}$ atomic $\text{m}^{-2}$ year $^{-1}$ )	$^{127}\text{I}$ deposition ( $\times 10^{18}$ atomic $\text{m}^{-2}$ year $^{-1}$ )	Refs.
1	Denmark and Sweden (55°N–68°N)	2000–2006	Rain water	(0.3–30)	(1.6–7.0)	Aldahan et al. (2009)
2	Sweden (56°N–68°N)	2001–2005	Rain water Aerosol	(0.3–3) (0.008–0.7)	(1.6–8.5) (0.03–3)	Englund et al. (2010)
3	Switzerland (Dübendorf/Zürich)	1994–1997	Rain water	(1.1–2.6)		Schnabel et al. (2001)
4	North America Alaskan and Canadian rivers	1996	River water	(0.001–0.004)		Moran et al. (2002)
	US West Coast rivers	1995–1997	River water	(0.00008–0.05)		
	US South Coast rivers	1995–1996	River water	(0.00002–0.03)		
	US East Coast rivers	1995–1996	River water	(0.02–7.3)		
5	Yukon Territory (Canada, 60°N–67°N)	2010	River water	(0.003–0.008)		Herod et al. (2013)
6	Norfolk (UK)	1996–1997	Rain water Aerosol		1.6 (2.2–4.0)	Baker et al. (2001)
7	Europe Germany (Ammersee, Bodensee, Chiemsee) Italy (Como, Garda, Geneva, Lugano, Maggiore)	1998–2004 1998–1999	Lake water Lake water	(0.6–3.8) (1.1–9.3)		Reithmeier et al. (2007)
8	Denmark (Roskilde)	2001–2004	Rain water	(0.9–1.5)	(2.8–6.1)	Hou et al. (2009)
9	Asia Russia (Ladoga, Onega, Ilmen, Baikal) Kyrgyzstan (Issyk Kull) Mongolia (Khuvsgul)	1999–2001 2004 2001	Lake water Lake water Lake water	(0.3–25) 16.2 3.2		Reithmeier et al. (2010)
	Africa Malawi (Malawi) Tanzania (Victoria)	2001 2001	Lake water Lake water	0.16* 0.14		
	America Argentina (Nahuel Huapi) Peru (Titicaca) USA (Wonder lake, Alaska)	2002 2000 2002	Lake water Lake water Lake water	9.0 0.16 1.6*		
	Oceania New Zealand (Rotorua, Taupo)	2003	Lake water	0.65*		
10	Arctic Sea (Eurasian, Amundsen and Makarov basins)	2007	Sea ice	(3.6–20)	(2.6–8.6)	This work

ing facilities would have reached the Arctic Ocean and presently resides in the upper 1000 m of the water column.

Recent studies (Karcher et al., 2012; Smith et al., 2011) have determined  $^{129}\text{I}$  concentrations in surface waters ( $\leq 10$  m depth) of the Arctic Ocean sampled in 2007 during the same expedition ARK XXII/2-IPY-SPACE. Excluding two samples collected in the Laptev Sea, far away from our sampling stations, the  $^{129}\text{I}$  concentrations in surface seawater ranged from  $23 \times 10^7$  to  $606 \times 10^7$  atoms  $\text{L}^{-1}$ , with a mean value of  $(335 \pm 210) \times 10^7$  atoms  $\text{L}^{-1}$ .

Algae can concentrate iodine to a high level, with concentration factors as high as  $10^4$  (Hou and Yan, 1998). The greatest fraction of sea ice algae often reside in the bottom 2–10 cm of the ice floes, where despite the low light intensities (as low as 0.1% of the

incoming irradiance) the nutrient supply coming from the underlying water supports growth (Michel et al., 2006; Cota et al., 1987). Iodine could then also be incorporated from the water column by sea ice algae. Then, the maximum inventory of  $^{129}\text{I}$  in seawater that could be incorporated by sea ice due to marine algae could be estimated by multiplying the average concentration of  $^{129}\text{I}$  in surface seawater,  $(335 \pm 210) \times 10^7$  atoms  $\text{L}^{-1}$  (Karcher et al., 2012; Smith et al., 2011), by the depth of the Arctic mixed layer (12–32 m) (Cámara-Mor et al., 2011) at the sampling stations occupied during this cruise, giving a range of  $(40–107) \times 10^{12}$  atoms  $\text{m}^{-2}$  and a mean value of  $(74 \pm 48) \times 10^{12}$  atoms  $\text{m}^{-2}$ . The same calculation can be performed for  $^{127}\text{I}$  using concentrations measured by Michel et al. (2012) for surface seawater (2 and 9 m depth,

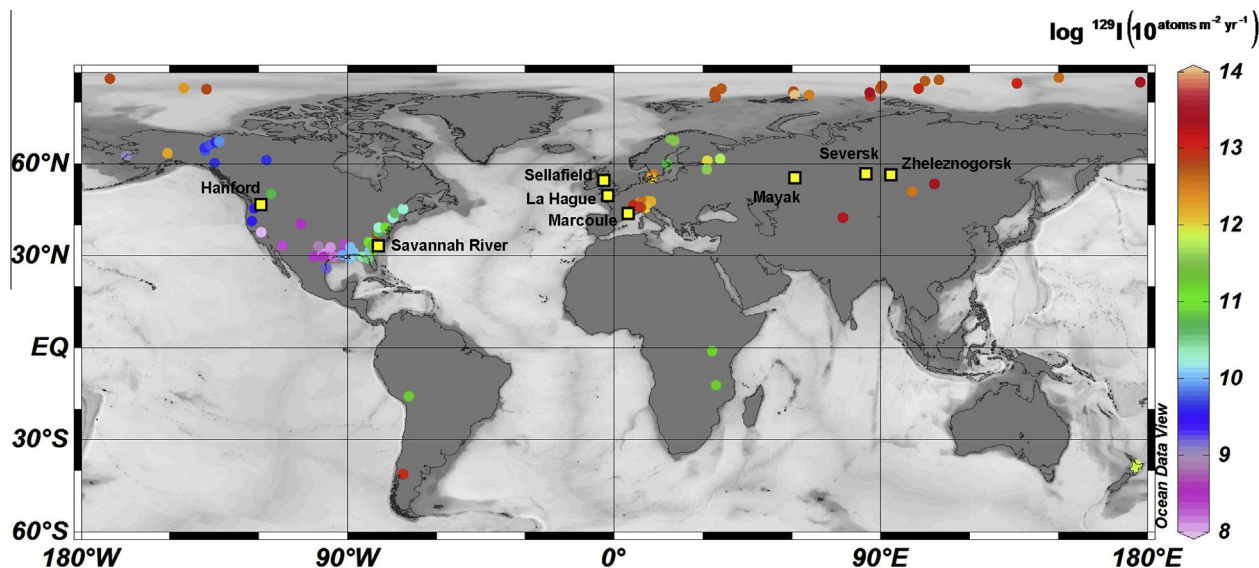


**Fig. 4.** Geographical distribution and  $^{129}\text{I}$  concentrations of sampling sites listed in Table 2 (circles) and major  $^{129}\text{I}$  sources, i.e. the European (Sellafield, La Hague, Marcoule), former Soviet (Mayak, Seversk, Zheleznogorsk) and US (Hanford, Savannah River) reprocessing facilities (squares).

respectively) at the coast of Spitsbergen ( $38$  and  $36 \text{ ng g}^{-1}$ ), giving an inventory range for  $^{127}\text{I}$  in the mixed layer of  $2.1$  to  $5.6 \times 10^{21} \text{ atoms m}^{-2}$ , with a mean value of  $3.4 \times 10^{21} \text{ atoms m}^{-2}$ . Those two results lead us a mean  $^{129}\text{I}/^{127}\text{I}$  ratio in the Arctic mixed layer of  $(2.2 \pm 1.4) \times 10^{-8}$ .

During the warm months, the extent of sea ice in the Arctic basin is reduced by a factor of approximately 2 (for the period 1979–2000; NSIDC). This fact would lead to a potential inventory of  $^{129}\text{I}$  of  $(3.2 \pm 2.2) \times 10^{12} \text{ atoms m}^{-2}$  being available for the surface water. Assuming that the iodine atoms were rapidly released at the central Arctic area, such a yearly contribution to the Arctic mixed layer would be in the range of 4% of the Arctic mixed layer inventory. Thus, this contribution has been neglected.

#### 4.3. Iodine release from sea ice to the Arctic atmosphere

The transfer mechanisms of iodine from the ocean into the atmosphere are not fully understood, and can depend on solar radiation, ocean water temperature and chemistry, biological activity (micro- and macro-algae), physical parameters (waves, tides and currents), and spatial extend (open sea/coastal areas and water depth) (Bell et al., 2002). Volatilization and photooxidation of organo-iodines in air to soluble inorganic forms allow for a significant fraction of the iodine to partition to the aerosol phase, providing a route for wet and dry deposition to the ocean (Carpenter, 2003). Apart from volatilization, inorganic sources of iodine ( $\text{I}_2$  and/or HOI) in the polar atmosphere have also been suggested (Saiz-López and Boxe, 2008).  $\text{I}_2$  may be formed at the ocean (and ice) surface by the reaction of iodide with ozone or photo-oxidation by chlorophyll. Iodine may then be volatilized to the atmosphere directly, or react with organic compounds to yield iodocarbons. Another suggested source of inorganic iodine to the atmosphere is the biological production of  $\text{I}^-$  and HOI from marine algae contained within and underneath sea ice, and their diffusion through brine channels to accumulate on the surface brine layer resulting in the release of  $\text{I}_2$ ,  $\text{ICl}$  and/or  $\text{IBr}$  to the atmosphere (Saiz-López and Boxe, 2008).

Iodine release from the sea ice is triggered by the biological production of iodine, in the equilibrium form of  $\text{HOI} + \text{I}^- + \text{H}^+ \rightarrow \text{I}_2 + \text{H}_2\text{O}$  from sea ice algae followed by diffusion through brine channels to accumulate in the QLL (Quasi-Liquid Layer) of the ice surface accompanied by deposition and recycling of atmospheric iodine

species on the QLL, as shown in Figs. 1 and 2 of Saiz-López and Boxe (2008). Simulations reported by Saiz-López and Boxe (2008) show that the nocturnal gas-phase  $\text{I}_2$  can reach concentrations of  $7 \times 10^8 \text{ molecules cm}^{-3}$  over the course of six days, whereas daytime  $\text{I}_2$  concentrations are much smaller due to rapid photolysis to form I atoms. Thus, an upper limit for the amount of  $^{127}\text{I}$  released from the sea ice by this mechanism could be estimated as the product of the nocturnal gas-phase  $\text{I}_2$  ( $7 \times 10^8 \text{ molecules cm}^{-3}$ ), and the QLL thickness ( $500 \mu\text{m}$ ) (Saiz-López and Boxe, 2008), leading to a total amount of  $7 \times 10^{11} \text{ atoms m}^{-2}$  of  $^{127}\text{I}$  released from the sea ice.

Taking the mean  $^{129}\text{I}/^{127}\text{I}$  atom ratio in sea ice of  $(1.2 \pm 1.7) \times 10^{-6}$ , this would correspond to an amount of  $^{129}\text{I}$  released from the sea ice of  $(8.5 \pm 12.0) \times 10^5 \text{ atoms m}^{-2}$ . This amount of  $^{129}\text{I}$  volatilised is negligible in comparison with the  $^{129}\text{I}$  inventory in sea ice calculated above, of  $(6.5 \pm 4.5) \times 10^{12} \text{ atoms m}^{-2}$ . The same occurs with the amount of  $^{127}\text{I}$  that is volatilised from sea ice ( $7 \times 10^{11}$  vs  $(5.5 \pm 4.0) \times 10^{18} \text{ atoms m}^{-2}$ ).

#### 4.4. Origin of iodine in Arctic sea ice

The inventories of  $^{129}\text{I}$  and  $^{127}\text{I}$  in sea ice can be considered as a balance of their mass exchanges between the sea ice and the ocean and atmosphere. Iodine has a fairly short atmospheric residence time of  $(12 \pm 3)$  days (Yang and Guo, 2012) and emission of organic iodide from the ocean provides the main source of atmospheric  $^{127}\text{I}$ . Anthropogenic releases of atmospheric  $^{127}\text{I}$  (such as fossil fuel combustion) are believed to be negligible on the global scale compared to natural, oceanic sources (Carpenter, 2003). However, the  $^{129}\text{I}/^{127}\text{I}$  ratio of  $(1.2 \pm 1.7) \times 10^{-6}$  in sea ice is much higher compared to that for the surrounding seawater of  $(2.2 \pm 1.4) \times 10^{-8}$  indicating that the  $^{129}\text{I}$  inventory in sea ice cannot be supported by direct uptake from seawater or by iodine emission from proximal (nearby) oceanic regimes.

To address this issue it is assumed that there are two sources for the  $^{129}\text{I}$  inventory,  $^{129}\text{I}_{\text{sea-ice}}^{\text{total}}$ , in sea ice: (1) emission from the proximal ocean and subsequent deposition in sea ice resulting in a seawater-derived, ice inventory of  $^{129}\text{I}_{\text{sea-ice}}^{\text{wat}}$ , and (2) direct atmospheric transport from European nuclear reprocessing plants (Sellafield in the UK and Cap La Hague in France) followed by deposition in sea ice, giving a long range atmospherically-derived com-



ponent of  $^{129}\text{I}_{\text{sea-ice}}^{\text{atm}}$ . One can further assume that the total  $^{127}\text{I}$  inventory in the Arctic sea ice of  $^{127}\text{I}_{\text{sea-ice}}^{\text{total}}$  comes solely from ocean emission, because land-based sources of  $^{127}\text{I}$  are minor compared to ocean sources. The  $^{129}\text{I}$  inventory in sea ice derived from ocean emission is then as follows,

$$^{129}\text{I}_{\text{sea-ice}}^{\text{wat}} = ^{127}\text{I}_{\text{sea-ice}}^{\text{total}} \cdot \left( \frac{^{129}\text{I}}{^{127}\text{I}} \right)_{\text{water}} \quad (1)$$

where  $(^{129}\text{I}/^{127}\text{I})_{\text{water}}$  is the iodine isotopic ratio in seawater ( $2.2 \times 10^{-8}$ ; Section 4.2) and  $^{127}\text{I}_{\text{sea-ice}}^{\text{total}}$  is  $5.5 \times 10^{18}$  atoms  $\text{m}^{-2}$  (Section 4.1) giving a value for  $^{129}\text{I}_{\text{sea-ice}}^{\text{wat}}$  of  $(1.2 \pm 1.7) \times 10^{11}$  atoms  $\text{m}^{-2}$ . Therefore, the amount of  $^{129}\text{I}$  derived from long range transport from European nuclear reprocessing plants  $^{129}\text{I}_{\text{sea-ice}}^{\text{atm}}$  is the difference,  $^{129}\text{I}_{\text{sea-ice}}^{\text{total}} - ^{129}\text{I}_{\text{sea-ice}}^{\text{wat}}$ , equal to  $(6.4 \pm 4.7) \times 10^{12}$  atoms  $\text{m}^{-2}$  or 98.4% of the total  $^{129}\text{I}$  inventory in the Arctic sea ice.

This result suggests that most of the  $^{129}\text{I}$  measured in sea ice in this study was derived from long range transport to the Arctic Ocean from the vicinity of Sellafield and La Hague and/or remote oceanic regions having very high  $^{129}\text{I}$  concentrations. To test this hypothesis, an air parcel trajectory analysis was performed using the National Oceanic and Atmosphere Administration (NOAA) Hybrid Single-Particle Lagrangian Integrated Trajectory (HYSPPLIT) atmospheric transport/dispersion model, together with meteorological data spanning the relevant sampling periods. The model has been designed to support a wide range of simulations related to the atmospheric transport and dispersion of pollutants and hazardous materials to the Earth's surface, and it is used to track and forecast the releases of various substances to the atmosphere including radioactive materials, volcanic ash and wildfire smoke (Draxler and Rolph, 2003).

We have reconstructed five air mass pathways originating at Sellafield (red) and La Hague (blue) at different dates (as shown in Fig. 3) that cover the entire sampling period using the HYSPPLIT model. The modelling results confirm that these air parcels originating in the vicinity of Sellafield and La Hague could reach the sampling area at the time of sampling and that, in some cases, the air mass also passed through the Baltic and North Seas. This would explain the fact that 98.4% of the total  $^{129}\text{I}$  inventory in the Arctic sea ice comes from direct atmospheric transport from the European nuclear reprocessing plants or through emission in remote oceanic regions (ie. Baltic and North Seas) having very high water column  $^{129}\text{I}$  concentrations.

#### 4.5. Iodine atmospheric deposition rates

The measured inventory of iodine in the Arctic sea ice can be used to calculate the atmospheric deposition rates by making an assumption about the "age" of the sea ice samples. Since the floes sampled for this work were approximately one year old or even younger (Cámara-Mor et al., 2010, 2011), then the (net) atmospheric deposition rates for  $^{129}\text{I}$  and  $^{127}\text{I}$  in the Arctic sea ice would be of  $(6.5 \pm 4.5) \times 10^{12}$  atoms  $\text{m}^{-2} \text{year}^{-1}$  and  $(5.5 \pm 4.0) \times 10^{18}$  atoms  $\text{m}^{-2} \text{year}^{-1}$ , respectively. A comparison of  $^{129}\text{I}$  and  $^{127}\text{I}$  deposition rates from other global locations is shown in Table 2. Fig. 4 illustrates the geographical distribution of the  $^{129}\text{I}$  data given in Table 2 including the major  $^{129}\text{I}$  sources associated with European (Sellafield, La Hague, Marcoule), former Soviet (Mayak, Seversk, Zheleznogorsk) and US (Hanford, Savannah River) reprocessing facilities.

Aldahan et al. (2009) have reported wet deposition rates for both isotopes in the period 2000–2006 at European latitudes (55°N–68°N), ranging  $(0.3\text{--}30) \times 10^{12}$  atoms  $\text{m}^{-2} \text{year}^{-1}$  for  $^{129}\text{I}$  and  $(1.6\text{--}7.0) \times 10^{18}$  atoms  $\text{m}^{-2} \text{year}^{-1}$  for  $^{127}\text{I}$ . Their results indicate variability for both isotopes associated with generally higher values at near coastal sites compared to the inland ones. Back tra-

jectories calculated through assigning a region of origin for each precipitation event revealed that air masses had passed over the Sellafield/La Hague/North Sea area 3 days before the precipitation event took place. Englund et al. (2010) have also reported wet deposition rates of  $^{129}\text{I}$  and  $^{127}\text{I}$  in the period 2001–2005 in two localities in Sweden (Northern and Southern) ranging  $(0.3\text{--}3) \times 10^{12}$  atoms  $\text{m}^{-2} \text{year}^{-1}$  for  $^{129}\text{I}$  and  $(1.6\text{--}8.5) \times 10^{18}$  atoms  $\text{m}^{-2} \text{year}^{-1}$  for  $^{127}\text{I}$ . The correlation found between both isotopes suggested that they originate from a common source, likely the North Sea; in the case of  $^{129}\text{I}$ , due to volatilization of liquid emissions from the reprocessing facilities in Sellafield and La Hague.

Schnabel et al. (2001) reported  $^{129}\text{I}$  wet deposition fluxes in rain water samples collected in Switzerland between 1994–1997, ranging  $(1.1\text{--}2.6) \times 10^{12}$  atoms  $\text{m}^{-2} \text{year}^{-1}$ . They concluded that the two main sources of  $^{129}\text{I}$  in precipitation in central Europe are the transfer of the liquid  $^{129}\text{I}$  released by Sellafield and La Hague reprocessing plants from the sea to the atmosphere and the gaseous  $^{129}\text{I}$  releases from the same plants. Similar  $^{129}\text{I}$  deposition fluxes have been reported by Reithmeier et al. (2007) in Germany and Italy, ranging  $(0.6\text{--}9.3) \times 10^{12}$  atoms  $\text{m}^{-2} \text{year}^{-1}$  in lake water samples collected between 1998 and 2004.

Reithmeier et al. (2010) calculated the  $^{129}\text{I}$  deposition fluence up to 2004 due to gaseous releases from all facilities shown in Fig. 4 of this manuscript by using a transport model based on modelling the  $^{129}\text{I}$  released from those reprocessing plants. Using the estimated from Reithmeier et al. (2010) (ie. Fig. 3 in that paper), we can infer deposition fluxes of about  $5 \times 10^{13}$  atoms  $\text{m}^{-2}$  in the Arctic Ocean. Since the first facility started to operate in 1948, this would correspond to an average annual deposition of about  $1 \times 10^{12}$  atoms  $\text{m}^{-2} \text{year}^{-1}$ , in good agreement with the results shown in our study.

The results for  $^{129}\text{I}$  fluxes in the Yukon territory (Canada) reported by Herod et al. (2013) are much lower than those reported in central Europe, ranging  $(0.003\text{--}0.008) \times 10^{12}$  atoms  $\text{m}^{-2} \text{year}^{-1}$ , due to the remoteness of the region and the lack of nearby  $^{129}\text{I}$  point sources. The same applies to other remote sampling locations in the southern hemisphere, like New Zealand (lakes Rotorua and Taupo) or Africa (lakes Malawi and Tanzania), where data reported by Reithmeier et al. (2010) show low  $^{129}\text{I}$  deposition fluxes which would be essentially due to fallout from the atmospheric nuclear explosions. The main exception is a relatively high  $^{129}\text{I}$  deposition flux of  $9.0 \times 10^{12}$  atoms  $\text{m}^{-2} \text{year}^{-1}$  determined from measurements performed in lake Nahuel Huapi (Argentina).  $^{129}\text{I}$  deposition fluxes in rivers from North America reported by Moran et al. (2002) are in general rather low, in the range  $(0.00002\text{--}0.05) \times 10^{12}$  atoms  $\text{m}^{-2} \text{year}^{-1}$ . These results indicate that  $^{129}\text{I}$  fallout from atmospheric test explosions is the only source and that  $^{129}\text{I}$  releases from the US reprocessing facilities is negligible. The sole exception is a higher  $^{129}\text{I}$  deposition flux ranging  $(0.02\text{--}7.3) \times 10^{12}$  atoms  $\text{m}^{-2} \text{year}^{-1}$  on the Southeast coast due to the gaseous emissions of the Savannah River plant.

The published data for  $^{127}\text{I}$  deposition fluxes is comparatively sparse.  $^{127}\text{I}$  wet deposition fluxes reported in the northern hemisphere (Table 2) are in the range  $(1.6\text{--}8.6) \times 10^{18}$  atoms  $\text{m}^{-2} \text{year}^{-1}$  (Baker et al., 2001) with generally higher values being measured at coastal sites compared to inland ones.

## 5. Conclusions

Concentrations of  $^{129}\text{I}$  in surface sea ice samples from the central Arctic Ocean collected in 2007 ranged between  $(98 \pm 8) \times 10^7$  atoms  $\text{L}^{-1}$  to  $(1327 \pm 116) \times 10^7$  atoms  $\text{L}^{-1}$ , with an average value of  $(378 \pm 292) \times 10^7$  atoms  $\text{L}^{-1}$ . The  $^{129}\text{I}$  inventory in the sea ice was estimated as  $(6.5 \pm 4.5) \times 10^{12}$  atoms  $\text{m}^{-2}$ . The two main sources for  $^{129}\text{I}$  in Arctic sea ice are: (1) emission from the ocean and subsequent deposition in sea ice; and (2) direct atmospheric

transport from the European nuclear reprocessing plants (Sellafield in the UK and Cap La Hague in France) or through emission in remote oceanic regions having very high  $^{129}\text{I}$  concentrations (eg. North Sea) followed by deposition in sea ice. Our data, supported by air parcel trajectory analysis for the sampling period, indicate that long range, atmospheric transport contributes most (up to 98.4%) of the total  $^{129}\text{I}$  present in the Arctic sea ice. The results shown in this work will serve as a basis for future sampling campaigns and warranties future research about  $^{129}\text{I}$  behaviour in the Arctic area.

## Acknowledgements

This work was partially funded by the Ministerio de Educación y Ciencia (MEC) of Spain (POL2006-00449), the prize ICREA Academia, funded by the Generalitat de Catalunya (PM), and the fellowship AP2006-03071 (PC-M). The authors are thankful to H. Reithmeier for fruitful discussions on his model of dispersion of  $^{129}\text{I}$  in the atmosphere. We are also thankful to the captain, crew and technicians of the R/V Polarstern and of Heliservice International GmbH for assistance during ARK XXII-2 cruise and to Servicio de Radioisótopos (University of Seville) for the technical support in the measurement of  $^{127}\text{I}$  concentration in the sea ice samples. PM was supported in part by a Gledden Visiting Fellowship awarded by the Institute of Advanced Studies at The University of Western Australia.

## References

- AMAP, 2004. AMAP Assessment 2002: radioactivity in the Arctic. Technical Report, Oslo, Norway
- Aagaard, K., 1981. On the deep circulation of the Arctic Ocean. *Deep-Sea Res.* 28, 251–268.
- Aldahan, A., Alfimov, V., Possnert, G., 2007.  $^{129}\text{I}$  anthropogenic budget: major sources and sinks. *Appl. Geochem.* 22, 606–618.
- Aldahan, A., Persson, S., Possnert, G., Hou, X.L., 2009. Distribution of  $^{127}\text{I}$  and  $^{129}\text{I}$  in precipitation at high European latitudes. *Geophys. Res. Lett.* 36. <http://dx.doi.org/10.1029/2009GL037363>.
- Alfimov, V., Aldahan, A., Possnert, G., Winsor, P., 2004. Anthropogenic iodine-129 in seawater along a transect from the Norwegian coastal current to the North Pole. *Mar. Pollut. Bull.* 49, 1097–1104.
- Alfimov, V., Possnert, G., Aldahan, A., 2006. Anthropogenic-129 in the Arctic Ocean and Nordic Seas: numerical modelling and prognoses. *Mar. Pollut. Bull.* 52, 380–385.
- Alfimov, V., Aldahan, A., Possnert, G., 2013. Water masses and  $^{129}\text{I}$  distribution in the Nordic Seas. *Nucl. Inst. Meth. Phys. Res. B* 294, 542–546.
- Baker, A.R., Tunnicliffe, C., Jickells, T.D., 2001. Iodine speciation and deposition fluxes from the marine atmosphere. *J. Geophys. Res.* 106, 28743–28749.
- Barrie, L., Falck, E., Gregor, D., Iverson, T., Loeng, H., Macdonald, R., 1998. The influence of physical and chemistry processes on contaminant transport into and within the Arctic. AMAP assessment, 25–116.
- Bell, N., Hsu, L., Jacob, D.J., Schultz, M.G., Blake, D.R., Butler, J.H., King, D.B., Robert, J.M., Maier-Reimer, E., 2002. Methyl iodide: atmospheric budget and use as a tracer of marine convection in global models. *J. Geophys. Res.* 107, 4340.
- Brant, J., Christensen, J.H., Frohn, L.M., 2002. Modelling transport and deposition of caesium and iodine from the Chernobyl accident using the DREAM model. *Atmos. Chem. Phys.* 2, 397–417.
- Buraglio, N., Aldahan, A., Possnert, G., 1999. Distribution and inventory of  $^{129}\text{I}$  in the central Arctic Ocean. *Geophys. Res. Lett.* 26, 1011–1014.
- Buraglio, N., Aldahan, A., Possnert, G., 2000. Analytical techniques and applications of  $^{129}\text{I}$  in natural water. *Nucl. Inst. Meth. Phys. Res. B* 172, 518–523.
- Cámara-Mor, P., Masqué, P., García-Orellana, J., Cochran, J.K., Mas, J.L., Chamizo, E., Hanfland, C., 2010. Arctic Ocean sea ice drift origin derived from artificial radionuclides. *Sci. Tot. Environ.* 408, 3349–3358.
- Cámara-Mor, P., Masqué, P., García-Orellana, J., Kern, S., Cochran, J.K., Hanfland, C., 2011. Interception of atmospheric fluxes by Arctic sea ice: evidence from cosmogenic  $^7\text{Be}$ . *J. Geophys. Res.* 116, C12041.
- Carpenter, L.J., 2003. Iodine in the marine boundary layer. *Chem. Rev.* 103, 4953–4962.
- Casacuberta, N., Christl, M., Lachner, J., Rutgers van der Loeff, M., Masqué, P., Synal, H.-A., 2014. A first transect of  $^{236}\text{U}$  in the North Atlantic. *Geochim. Cosmochim. Acta* 133, 34–46.
- Cochran, J.K., Moran, S.B., Fisher, N.S., Beasley, T.M., Kelley, K.M., 2000. Sources and transport of anthropogenic radionuclides in the Ob river system. *Siberia. Earth Plan. Sci. Lett.* 179, 125–137.
- Cooper, L.W., Hong, G.H., Beasley, T.M., Grebmeier, J.M., 2001. Iodine-129 concentrations in marginal seas of the North Pacific and Pacific-influenced waters of the Arctic Ocean. *Mar. Pollut. Bull.* 42, 1347–1356.
- Cota, G.F., Prinsenberg, S.J., Bennett, E.B., Loder, J.W., Lewis, M.R., Anning, J.L., Watson, N.H.F., Harris, L.R., 1987. Nutrients fluxes during extended blooms of Arctic ice algae. *J. Geophys. Res.* 92, 1951–1962.
- Dahlgard, H., 1995. Transfer of European coastal pollution to the Arctic: radioactive tracers. *Mar. Pollut. Bull.* 31, 3–7.
- Draxler, R.R., Rolph, G.D., 2003. HYSPLIT (Hybrid Single-Particle Lagrangian Integrated Trajectory). NOAA Air Resources Laboratory, Silver Spring, MD. Model access via NOAA ARL READY Website. <http://ready.arl.noaa.gov/HYSPLIT.php>.
- Englund, E., Aldahan, A., Hou, X.L., Possnert, G., Söderström, C., 2010. Iodine ( $^{129}\text{I}$  and  $^{127}\text{I}$ ) in aerosols from Northern Europe. *Nucl. Inst. Meth. Phys. Res. B* 268, 1139–1141.
- Gallagher, D., McGee, E., Mitchell, P.I., Alfimov, V., Aldahan, A., Possnert, G., 2005. Retrospective search for evidence of the 1957 windscale fire in NE Ireland using  $^{129}\text{I}$  and other long-lived nuclides. *Environ. Sci. Technol.* 39, 2927–2935.
- Gascard, J.C., Raisbeck, G., Sequeira, S., Yiou, F., Mork, K.A., 2004. The Norwegian Atlantic Current in the Lofoten basin inferred from hydrological and tracer data ( $^{129}\text{I}$ ) and its interaction with the Norwegian Coastal current. *Geophys. Res. Lett.* 31, 01308.
- Gómez-Guzmán, J.M., López-Gutiérrez, J.M., Pinto-Gómez, A.R., Holm, E., 2012.  $^{129}\text{I}$  measurements on the IMV AMS facility at the Centro Nacional de Aceleradores (CNA, Spain). *Appl. Radiat. Isot.* 70, 263–268.
- He, P., Aldahan, A., Possnert, G., Hou, X.L., 2013. A summary of global  $^{129}\text{I}$  in marine waters. *Nucl. Inst. Meth. Phys. Res. B* 294, 537–541.
- Herod, M.N., Clark, I.D., Kieser, W.E., Agosta, S., Zhao, X.L., 2013.  $^{129}\text{I}$  dispersion and sources in Northwest Canada. *Nucl. Instr. Meth. Phys. Res. B* 294, 552–558.
- Hou, X.L., Yan, X.J., 1998. Study on the concentration and seasonal variation of inorganic elements in 35 species of marine algae. *Sci. Tot. Environ.* 222, 141–156.
- Hou, X.L., Aldahan, A., Nielsen, S., Possnert, G., 2009. Time series of  $^{129}\text{I}$  and  $^{127}\text{I}$  speciation in precipitation from Denmark. *Environ. Sci. Technol.* 43, 6522–6528.
- Karcher, M., Smith, J.N., Kauker, F., Gerdes, R., Smethie, W.M., 2012. Recent changes in Arctic Ocean circulation revealed by iodine-129 observations and modelling. *J. Geophys. Res.* 117, C08007.
- Kieser, W.E., Zhao, X.L., Soto, C.Y., Tracy, B., 2005. Accelerator mass spectrometry of  $^{129}\text{I}$ : technique and applications. *J. Radioanal. Nucl. Chem.* 263, 375–379.
- López-Gutiérrez, J.M., García-León, M., Schnabel, Ch., Suter, M., Synal, H.-A., Szidat, S., García-Tenorio, R., 2004. Relative influence of  $^{129}\text{I}$  sources in a sediment core from the Kattegat area. *Sci. Tot. Environ.* 323, 195–210.
- Maryon, R.H., Smith, F.B., Conway, B.J., Goddard, D.M., 1991. The U.K. nuclear accident model. *Prog. Nucl. Energy* 26, 85–104.
- Masqué, P., Cochran, J.K., Hebbeln, D., Hirschberg, D.J., Dethleff, D., Winkler, A., 2003. The role of sea ice in the fate of contaminants in the Arctic Ocean: plutonium atom ratios in the Fram Strait. *Environ. Sci. Technol.* 37, 4848–4864.
- Masqué, P., Cochran, J.K., Hirschberg, D.J., Dethleff, D., Hebbeln, D., Winkler, A., Pfirman, S., 2007. Radionuclides in Arctic sea ice: tracers of sources, fates and ice transit time scales. *Deep Sea Res.* 54, 1289–1310.
- Michel, C., Ingram, R., Harris, L., 2006. Variability in oceanographic and ecological processes in the Canadian Arctic Archipelago. *Prog. Oceanogr.* 71, 379–401.
- Michel, R., Darauoi, A., Gorny, M., Jakob, D., Sachse, R., Tosch, L., Nies, H., Goroncy, I., Herrmann, J., Synal, H.-A., Stocker, M., Alfimov, V., 2012. Iodine-129 and iodine-127 in European seawaters and precipitation from Northern Germany. *Sci. Tot. Environ.* 419, 151–169.
- Moran, J.E., Oktay, S.D., Santschi, P.H., 2002. Sources of iodine and iodine-129 in rivers. *Water Resour. Res.* 38, 1149.
- NSIDC, National Snow & Ice Data Center. [http://nsidc.org/news/newsroom/2014\\_seasonalseaice\\_PR.html](http://nsidc.org/news/newsroom/2014_seasonalseaice_PR.html).
- Orre, S., Smith, J.N., Alfimov, V., Bentsen, M., 2010. Simulating transport of  $^{129}\text{I}$  and idealized tracers in the northern North Atlantic Ocean. *Environ. Fluid Mech.* 10, 213–233.
- Pfirman, S.L., Kogeler, J.W., Rigor, I., 1997. Potential for rapid transport of contaminants from the Kara Sea. *Sci. Tot. Environ.* 202, 111–122.
- Raisbeck, G.M., Yiou, F., Zhou, Z.Q., Kilius, L.R., 1995.  $^{129}\text{I}$  from nuclear fuel reprocessing facilities at Sellafield (UK) and La Hague (France): potential as an oceanographic tracer. *J. Mar. Syst.* 6, 561–570.
- Reithmeier, H., Lazarev, V., Rühm, W., Nolte, E., 2007.  $^{129}\text{I}$  measurements in lake waters for an estimate of regional  $^{129}\text{I}$  depositions. *Sci. Tot. Environ.* 376, 285–293.
- Reithmeier, H., Lazarev, V., Rühm, W., Nolte, E., 2010. Anthropogenic  $^{129}\text{I}$  in the atmosphere: overview over major sources, transport processes and deposition pattern. *Sci. Tot. Environ.* 408, 5052–5064.
- Rigor, I.G., Wallace, J.M., Colony, R., 2002. Response of sea ice to the Arctic Oscillation. *J. Climate* 15, 2648–2663.
- Saiz-López, A., Boxe, C.S., 2008. A mechanism for biologically-induced iodine emissions from sea-ice. *Atmos. Chem. Phys. Discuss.* 8, 2953–2976.
- Schnabel, C., López-Gutiérrez, J.M., Szidat, S., Sprenger, M., Wernli, H., Beer, J., Synal, H.-A., 2001. On the origin of  $^{129}\text{I}$  in rain water near Zürich. *Radiochim. Acta* 89, 815–822.
- Smith, J., Ellis, K., Kilius, L., 1998.  $^{129}\text{I}$  and  $^{137}\text{Cs}$  tracer measurements in the Arctic Ocean. *Deep Sea Res.* 45, 959–984.
- Smith, J., Ellis, K., Boyd, T., 1999. Circulation features in the central Arctic Ocean revealed by nuclear fuel reprocessing tracers from Scientific Ice Expeditions 1995 and 1996. *J. Geophys. Res.* 104, 29663–29677.

- Smith, J.N., McLaughlin, F.A., Smethie Jr., W.M., Moran, S.B., Lepore, K., 2011. Iodine-129,  $^{137}\text{Cs}$  and CFC-11 tracer transit time distributions in the Arctic Ocean. *J. Geophys. Res.* 116, C04024.
- Snyder, G., Aldahan, A., Possnert, G., 2010. Global distribution and long-term fate of anthropogenic  $^{129}\text{I}$  in marine and surface water reservoirs. *Geochem. Geophys. Geosyst.* 11, Q04010.
- Suzuki, T., Kabuto, S., Amano, H., Togawa, O., 2008. Measurement of iodine-129 in seawater samples collected from the Japan Sea area using accelerator mass spectrometry: contribution of nuclear fuel reprocessing plants. *Quat. Geochr.* 3, 268–275.
- UNSCEAR, 2000. United Nations Scientific Committee on the effects of atomic radiation. Sources and effects of ionizing radiation, Vol. 1: Sources. Report to the General Assembly. United Nations, New York, pp 654.
- Wagner, M.J.M., Dittich-Hannen, B., Synal, H.A., Suter, M., Schotterer, U., 1996. Increase of  $^{129}\text{I}$  in the environment. *Nucl. Instr. Meth Phys. Res. B* 113, 490–494.
- Yang, W., Guo, L., 2012. Depositional fluxes and residence time of atmospheric radioiodine ( $^{131}\text{I}$ ) from the Fukushima accident. *J. Environ. Radiact.* 113, 32–36.